NASA TECHNICAL NOTE

NASA TN D-3435

NASA TN D-3435

JET-INDUCED LIFT LOSS OF JET VTOL CONFIGURATIONS IN HOVERING CONDITION

by H. Clyde McLemore

Langley Research Center
Langley Station, Hampton, Va.

NATIONAL AERONAUTICS AND SPACE ADMINISTRATION • WASHINGTON, D. C. • JUNE 1966

NASA TN D-3435

JET-INDUCED LIFT LOSS OF JET VTOL CONFIGURATIONS IN HOVERING CONDITION

By H. Clyde McLemore

Langley Research Center
Langley Station, Hampton, Va.

NATIONAL AERONAUTICS AND SPACE ADMINISTRATION

For sale by the Clearinghouse for Federal Scientific and Technical Information
Springfield, Virginia 22151 – Price $2.00

JET-INDUCED LIFT LOSS OF JET VTOL CONFIGURATIONS IN HOVERING CONDITION

By H. Clyde McLemore
Langley Research Center

SUMMARY

Jet-induced lift losses of jet VTOL configurations for hovering flight out of ground effect have been investigated by using a turbojet engine exhausting through a flat square base plate. The investigation was conducted in still air. Several base-plate sizes and nozzle configurations were investigated for a range of engine operating conditions from idle to maximum thrust. For single-exhaust-nozzle configurations the induced lift loss was about 0.5 percent of the total installed thrust and for a multiple-nozzle configuration the losses were about three times this value. It was found that the jet-induced lift losses of the large-scale turbojet-powered configuration could be adequately simulated by small-scale cold-jet models provided that the rate of decay of jet velocity downstream of the nozzle is simulated. It was also found that the lift losses could be calculated within about ±20 percent by means of an empirical expression based on the rate of decay of the jet velocity downstream of the nozzle.

INTRODUCTION

Previous research in the United States and abroad has shown that a significant jet-induced lift loss may occur, at zero wind conditions out of ground effect, on jet VTOL aircraft when the jet exhaust is directed through the bottom of the fuselage or wing lower surface. Most of this research has been done at small scale by using a stream of cold compressed air to simulate the turbojet engine exhaust, and lift losses of the order of 1 to 4 percent of the total engine thrust have been experienced (refs. 1 to 3). This research has shown that the number and arrangement of the jet exhaust nozzles are very significant factors. It has also been theorized in reference 3, on the basis of these small-scale cold-flow tests, that the turbulence in the jet exhaust would cause a lift loss because it influences the rate at which air beneath a jet VTOL aircraft is entrained by the jet flow and sucked away from the bottom of the airplane. It would therefore be expected that it would be important in investigating this base loss that the turbulence in the jet exhaust be properly simulated. It was also theorized and established in references 1 and 3 that the rate of decay of the jet downstream of the nozzle was a correlating factor

related to the rate of entrainment of the surrounding air and the consequent effect on lift loss.

Because of the importance of the lift loss on the payload of a jet VTOL aircraft, it was felt that lift-loss tests should be conducted at large scale by utilizing an actual jet-engine exhaust as the test medium for correlation with the results of the small-scale cold-flow tests. With this arrangement the exhaust turbulence, temperature, and impact pressure of an actual jet VTOL aircraft would be simulated at reasonably large scale, and the resulting lift loss would be the order of magnitude one could expect from an actual jet VTOL aircraft. Such tests and correlations have been made in the present investigation for a single-nozzle and a four-nozzle configuration with the nozzles exhausting through square flat base plates intended to represent the bottom of a VTOL airplane. The investigation was made for a range of base-plate sizes and jet pressure ratios.

SYMBOLS

A	nozzle area, centimeters^2
D	tailpipe diameter (cold), centimeters
D_e	effective diameter, diameter of circle having same area as total area of all nozzles of a multiple-jet configuration, centimeters
F	jet thrust, newtons
ΔL	load induced on plate, newtons
p_o	ambient static pressure, newtons/meter^2
p_r	total pressure measured at nozzle radius station r, newtons/meter^2
$p_{t,n}$	maximum total pressure measured at nozzle, newtons/meter^2
p_x	maximum total pressure at survey position x, newtons/meter^2
q_n	maximum impact pressure measured at nozzle, $(p_{t,n} - p_o)$, newtons/meter^2
q_r	impact pressure measured at nozzle radius station r, $(p_r - p_o)$, newtons/meter^2

q_x maximum impact pressure at survey position x, $(p_x - p_o)$, newtons/meter^2

R nozzle radius, centimeters

r nozzle radius station, centimeters

S area of flat plate, centimeters^2

T nozzle exhaust temperature, degrees Kelvin

x distance downstream from nozzle, centimeters

Subscripts:

i point of maximum rate of change of decay parameter

max maximum

MODEL AND APPARATUS

The model used in the investigation consisted of a J85 turbojet engine mounted in a horizontal plane exhausting through and normal to square flat plates of various size. The engine and plates were mounted on an engine test stand which was provided with a strain-gage system for measuring the combined load of the engine and plate system. The plates were attached to the test stand with a pin-ended joint at the bottom and were secured at the top with a strain gage for determining the plate loads. A sketch of this apparatus is shown in figure 1. The test stand was set up in the test chamber of the Langley full-scale tunnel in order that the tests might be made in a large enclosure relatively free of random wind and exhaust recirculation effects. The actual location of the apparatus and its dimensional relationship with the test area are shown in figures 2 and 3. Photographs of the setup for the four-nozzle configuration are given in figure 4.

The geometric characteristics of the tailpipes used in the investigation are shown in figure 5. These dimensions are for the ambient temperature conditions and must be corrected for temperature to correspond with the dimensions that exist during engine operation. The material of the tailpipes is 347 stainless steel, and the correction to the nozzle diameters taken from machine-design text books (e.g., ref. 4) is as follows: $\Delta D = 10.4 \times 10^{-6} \times \Delta T \times D$ where ΔD is the change in diameter in centimeters and ΔT is the change in temperature in degrees Fahrenheit. The resulting hot-nozzle diameters and areas for the tailpipe configurations are given in the following table:

Tailpipe configuration	Diameter, cm	Area, cm^2
Long single	31.20	766
Short single	31.40	776
Four nozzle:		
Each	15.75	195
Total effective	31.49	779

The geometric characteristics of the base plates used during the investigation are given in figure 6. The base plate of the short-tailpipe single-nozzle configuration shown is also representative of the long-tailpipe single-nozzle configuration.

The gap between the hot tailpipe and the aluminum nozzle alinement plate was approximately 0.3 cm for all tests. A fouling light was installed on the engine operator's instrument panel that showed whether the tailpipe touched the aluminum alinement plate, and, if fouling occurred, the aluminum plate was repositioned to provide the aforementioned 0.3-cm clearance.

The temperature and impact pressure of the jet exhaust at various distances downstream from the engine exhaust nozzle were obtained from a movable multiple-tube total-pressure—temperature rake. (See photographs of fig. 7.) A separate multiple-tube total-pressure rake was installed across the nozzle for determining the nozzle impact pressures. Only one nozzle of the four-nozzle configuration was surveyed. Temperatures of the nozzle conditions were determined from a hand-held temperature probe at the nozzle. Tailpipe temperature and pressure were measured by permanently mounted probes in the tailpipe.

METHODS AND TESTS

The tests were conducted on the floor of the Langley full-scale tunnel test chamber with the exhaust of the engine directed through a large 12.2-meter by 6.1-meter doorway into one of the tunnel return passages. (See fig. 2.) This procedure gives essentially still-air conditions for all tests. Of course there was some recirculation of air, but observations of wool tufts attached on and about the test apparatus showed the recirculation of air to be very low and of random velocity and direction. Tests were conducted at engine thrusts of 1780 newtons, 4448 newtons, and 7120 newtons corresponding to nozzle pressure ratios of approximately 1.1, 1.4, and 1.7, respectively.

The test procedure was to start the engine, stabilize the thrust at about 1780 newtons (idle), and record all data simultaneously. The engine revolution speed was then increased until the thrust was stabilized at about 4448 newtons and the data were again

recorded. The same procedure was followed for the final test condition. This procedure was used with each plate size and each tailpipe configuration and for each downstream survey position. The large multiple-tube total-pressure—temperature rake used for the downstream surveys was manually moved to a new position while the engine was inoperative.

The total-pressure probes for the rake and engine were connected to a multiple-tube mercury manometer which was referenced to ambient static pressure and photographically recorded. Temperatures were recorded on multiple-channel recording potentiometers.

RESULTS AND DISCUSSION

Lift-Loss Characteristics

The effects of nozzle geometry, plate size, and nozzle pressures on the jet-induced forces representing jet VTOL configurations out of ground effect are shown in figure 8. As pointed out previously, the lift-loss problem of jet VTOL aircraft in the hovering condition has been explored with small-scale cold-air jets, and the present investigation was made with the jet exhaust being furnished by an actual turbojet engine in order to provide information with a more realistic representation of all the important factors involved. The turbojet engine used in the tests is a relatively low-pressure-ratio engine, however, so that the maximum pressure ratio $\left(\frac{p_{t,n}}{p_o} = 1.73\right)$ is somewhat lower than might be desired. The tests were, therefore, made over a range of pressure ratios in order to establish the effects of pressure ratio and to permit extrapolation of the data with a reasonable degree of accuracy.

The jet-induced lift loss of a short-tailpipe single-nozzle configuration is presented in figure 8(a). These results show a lift loss of about 0.5 percent of the total engine thrust. The results also show that the lift loss is a function of area ratio but is not significantly affected by pressure ratio.

The results presented in figures 8(b) and (c) are for the long-tailpipe configurations. The long length of these tailpipes was not a desirable feature but was necessary in the test setup in order that the engine exhaust might be divided for the exhaust for the four-nozzle configuration; the long-tailpipe single-nozzle configuration was tested to afford a direct comparison. The results for the long-tailpipe single-nozzle configuration show that the jet-induced lift loss was of approximately the same magnitude as that of the short-tailpipe single-nozzle configuration but was much more affected by pressure ratio; however, significantly smaller lift losses were obtained at the higher pressure ratios for the long-tailpipe single-nozzle configuration. The results for the four-nozzle

configuration show the same trends as those for the long-tailpipe single-nozzle configuration except that the lift losses were about three times as great. These small values of lift loss are encouraging from a design viewpoint in that some small-scale unpublished investigations have shown values of jet-induced lift loss of about twice the values measured in the present investigation.

The reason for concern about tailpipe length in connection with the lift-loss results is that the results of some small-scale tests of a single-nozzle configuration in reference 1 had indicated that the lift loss was markedly affected by the turbulence in the jet exhaust flow. For example, for a ratio of plate area to nozzle area of about 70, the jet-induced lift loss varied from about 0.5 percent of the total thrust for a very smooth exhaust flow to about 3 percent for a very turbulent flow. It was not known whether the use of long tailpipes, as had been necessary for the four-nozzle arrangement, would have a significant effect on the jet turbulence and consequently on jet-induced lift loss. Although the level of turbulence was not measured directly, jet-exhaust flow profiles and downstream surveys, which will be presented subsequently, indicated that the turbulence level for the short tailpipe was somewhat higher than that for the long tailpipe. Apparently, however, this difference was not great enough to cause significant effects in the jet-induced lift loss since the general level of lift loss for the long and short single tailpipes was shown in figures 8(a) and 8(b) to be approximately the same.

Jet Decay Characteristics

The decay of temperature and impact pressure downstream of the nozzle for the configurations is shown in figures 9, 10, and 11, and a comparison of the impact-pressure decay characteristics of the three configurations at comparable pressure ratios is shown in figure 12. The data of reference 1 have indicated that the jet-induced lift loss is proportional to the rate of decay of the exhaust impact pressure and inversely proportional to the downstream distance that the maximum decay rate occurs. The data were therefore examined to determine whether these parameters correlated with the lift-loss characteristics of turbojet-engine configurations.

There are not enough test points to define the decay curves from the present investigation with sufficient accuracy for close correlation of the decay curves with the lift-loss data, but certain observations can be made. For example, the maximum rate of decay is much greater, and the downstream station at which it occurs is much smaller, for the four-nozzle configuration than for the single-nozzle configuration. This fact correlates with the fact that the lift loss is greater for the four-nozzle configuration. Also, the maximum rate of decay and the station at which it occurs is about the same for the long-tailpipe single-nozzle and the short-tailpipe single-nozzle configurations, and these facts correlate with the fact that these two configurations had about the same lift loss. Further, the maximum lift losses of figure 8 correlate within about ±20 percent

with that calculated by using the decay curves of figure 12 and the following empirical expression of reference 1:

$$\frac{\Delta L}{F} = -0.009\sqrt{\frac{S}{A}}\sqrt{\frac{\left[\frac{\partial(q_x/q_n)}{\partial(x/D_e)}\right]_{max}}{(x/D_e)_i}}$$

The exhaust impact-pressure characteristics of the configurations are shown in figures 13 and 14 for several downstream locations. The single-nozzle configurations (fig. 13) are seen to have very nonuniform flow across the nozzle with a large reduced pressure area in the center of the nozzle. This low-velocity region in the center of the jet exhaust might be the result of a low-velocity boundary layer that builds up along the conical fairing of the turbine hub or perhaps of flow separation from the hub fairing. It is also interesting to note that the flow from the four-nozzle configuration is beginning to merge, or coalesce, between the more closely spaced nozzles (fig. 14(a)) at about 4 effective diameters behind the nozzle, whereas, for the more widely spaced nozzles (fig. 14(b)), the flow has almost entirely decayed before the flow merges at 12 to 16 effective diameters.

Comparison With Small-Scale Data

To obtain a comparison of cold-exhaust, small-scale data with that of the subject investigation, the results of the present tests are compared in figure 15 with the unpublished results of tests of a 0.12-scale model of the subject exhaust nozzle configurations. Cold air was used as the test medium for the 0.12-scale model. Unfortunately, directly comparable pressure ratios were not investigated, but it is felt that some comparison can be made from these data. For the single-nozzle configurations, both sets of results in figure 15(a) show a similar low level of lift loss, but the small-scale cold-flow tests appear to overestimate the lift loss by about 0.3 percent of the total thrust as compared with an extrapolation of the results of the large-scale hot-gas tests to a comparable pressure ratio. For the four-nozzle configurations of figure 15(b), an extrapolation of the large-scale hot-gas data to the pressure ratio of the small-scale cold-flow tests would indicate that the four-nozzle cold jet would very closely predict the actual lift losses associated with an actual turbojet configuration. The correlation shown in figure 15 may be fortuitous, however, since no exhaust decay rates were available for the small-scale configurations to indicate whether the large- and small-scale results should have been expected to agree closely.

The results of the present investigation are further compared with small-scale cold-jet results of reference 1 in figures 16 and 17 for models for which the characteristics of the jet flow are better defined. The lift-loss characteristics of the single- and

four-nozzle configurations are not very similar with regard to nozzle impact-pressure profile, but, in spite of this difference, the lift-loss characteristics correlate fairly well on the basis of the exhaust decay characteristics. For example, the exhaust decay rate of the large-scale long-tailpipe single-nozzle configuration is very similar to that of the small-scale single-nozzle configuration of reference 1, and the lift-loss values are also approximately equal. (See figs. 16(b) and 16(c).) For the four-nozzle configurations shown in figure 17, the small-scale data show the exhaust flow to decay much more rapidly than that of the large-scale data and show an accompanying larger value of induced lift loss.

Although the foregoing correlation is limited and consequently far from conclusive, it indicates that small-scale cold-flow tests can be used to predict the lift loss of large-scale jet VTOL configurations with hot exhaust if the rate of decay of the jet impact pressure downstream of the nozzles is similar.

Comparison of Calculated and Measured Engine-Exhaust Decay

Since representation of the engine-exhaust decay seems to be an important factor in model tests to determine the jet-induced lift loss for VTOL aircraft, it is necessary to know this characteristic for the full-scale engines under consideration. In the design stage of aircraft development, however, the engines under consideration may not have been built or tested; hence their decay rate cannot be measured. It might then be important to know how well the engine-exhaust decay rate can be estimated. Consequently, the manufacturer's estimated exhaust decay rate taken from the installation manual for the engine of the present investigation is compared in figure 18 with the measured characteristics of the engine with the short-tailpipe single-nozzle configuration. This figure shows the variation of impact pressure with distance downstream of the nozzle as measured in the present investigation. (See fig. 12.) The short-tailpipe single nozzle was the one most representative of the normal exhaust nozzle of the engine. Presented also for comparison is an ideal curve for a smooth nonturbulent jet calculated by the method presented in reference 5.

The comparison presented in figure 18 shows that the manufacturer's estimate and the ideal values are very nearly the same for the lower pressure-ratio data; however, neither predicts the actual exhaust decay rate very well. For the higher pressure ratio, which is the condition of greater interest, the experimental results are well predicted by the manufacturer. The calculated results do not define the actual exhaust decay curve very well, but the correlation is better than that obtained for the lower pressure ratio and suggests that pressure ratios greater than 1.7 may be adequately predicted by theory.

CONCLUDING REMARKS

An investigation made at large scale with a turbojet engine to investigate the jet-induced lift losses associated with jet VTOL airplane configurations in the hovering condition out of ground effect has indicated on the basis of limited correlations that small-scale, cold-jet model tests can be used to determine the jet-induced lift losses of similar turbojet-powered VTOL aircraft configurations. The large-scale hot-jet lift-loss results correlated reasonably well with small-scale cold-jet results provided that the jets had a similar rate of decay of jet velocity downstream of the nozzle. The large-scale hot-jet lift-loss results also correlated within about ±20 percent with an empirical expression which was devised in NASA TN D-3166 for lift loss and which was based on jet-velocity decay curves of a small-scale cold jet.

The jet-induced lift losses associated with a single-nozzle configuration were found to be low (about 0.5 percent of the total installed thrust), and a multiple-jet-nozzle configuration experienced jet-induced lift losses about three times as great as those of the single-nozzle configurations.

Langley Research Center,
National Aeronautics and Space Administration,
Langley Station, Hampton, Va., March 17, 1966.

REFERENCES

1. Gentry, Garl L.; and Margason, Richard J.: Jet-Induced Lift Losses on VTOL Configurations Hovering In and Out of Ground Effect. NASA TN D-3166, 1966.

2. Davenport, Edwin E.; and Spreemann, Kenneth P.: Thrust Characteristics of Multiple Lifting Jets in Ground Proximity. NASA TN D-513, 1960.

3. Kuhn, Richard E.; and McKinney, Marion O., Jr.: NASA Research on the Aerodynamics of Jet VTOL Engine Installations. Presented at the AGARD Specialist Meeting on Aerodynamics of Power Plant Installation (Tullahoma, Tenn.), AGARD, Oct. 25-27, 1965.

4. Marks, Lionel S., ed.: Mechanical Engineers' Handbook. Fifth ed., McGraw-Hill Book Co., Inc., 1951, p. 278.

5. Küchemahn, Dietrich; and Weber, Johanna: Aerodynamics of Propulsion. McGraw-Hill Book Co., Inc., 1953.

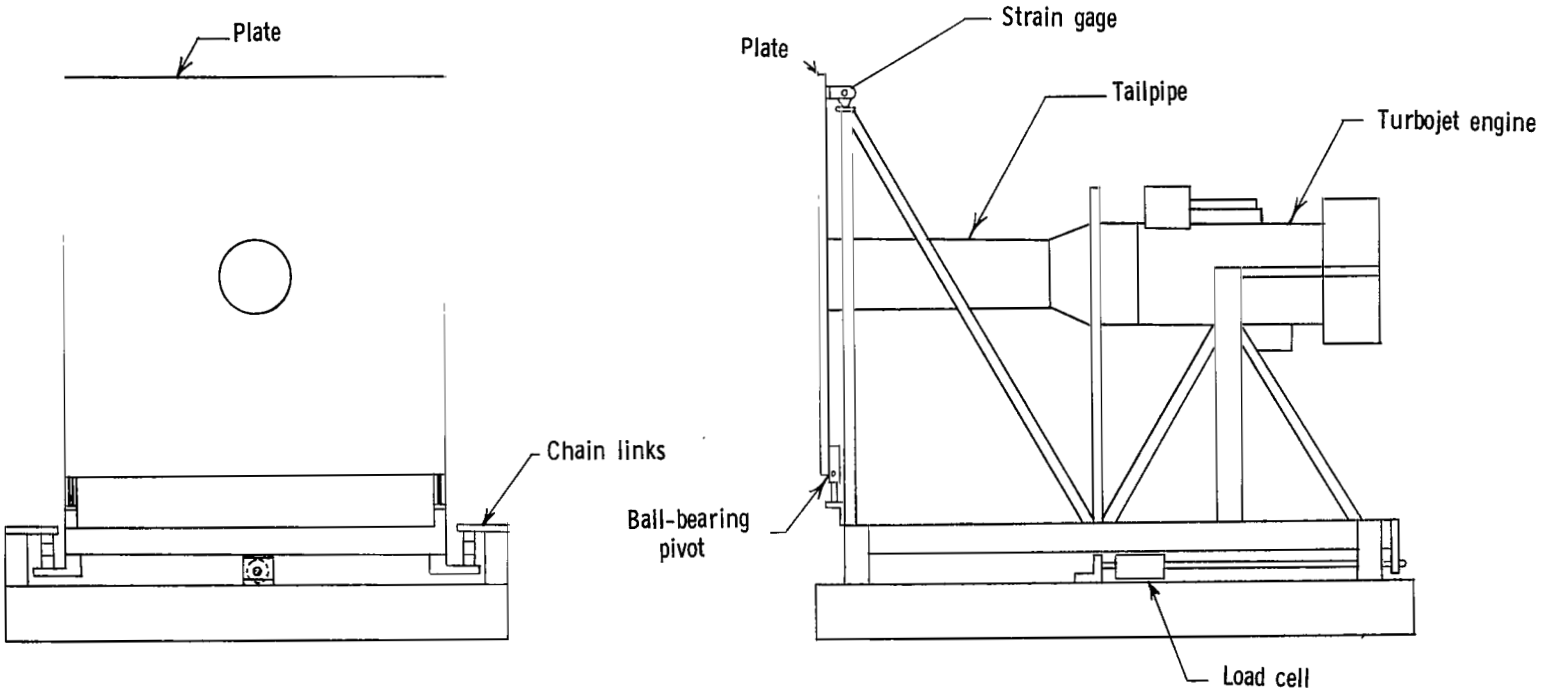

Figure 1.- Schematic drawing of test apparatus.

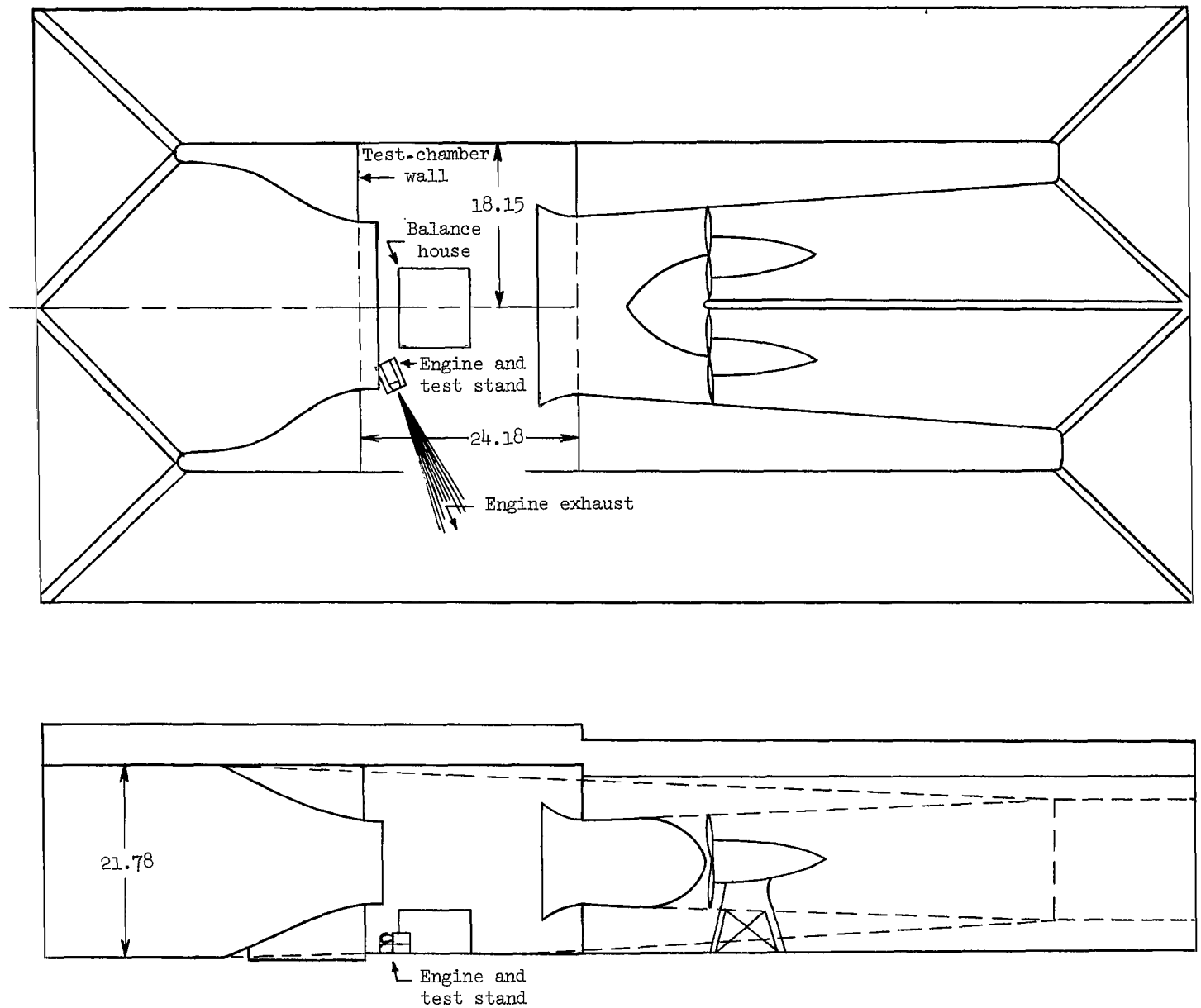

Figure 2.- Plan and elevation sketch of Langley full-scale tunnel showing location of turbojet engine and test stand. Dimensions are in meters.

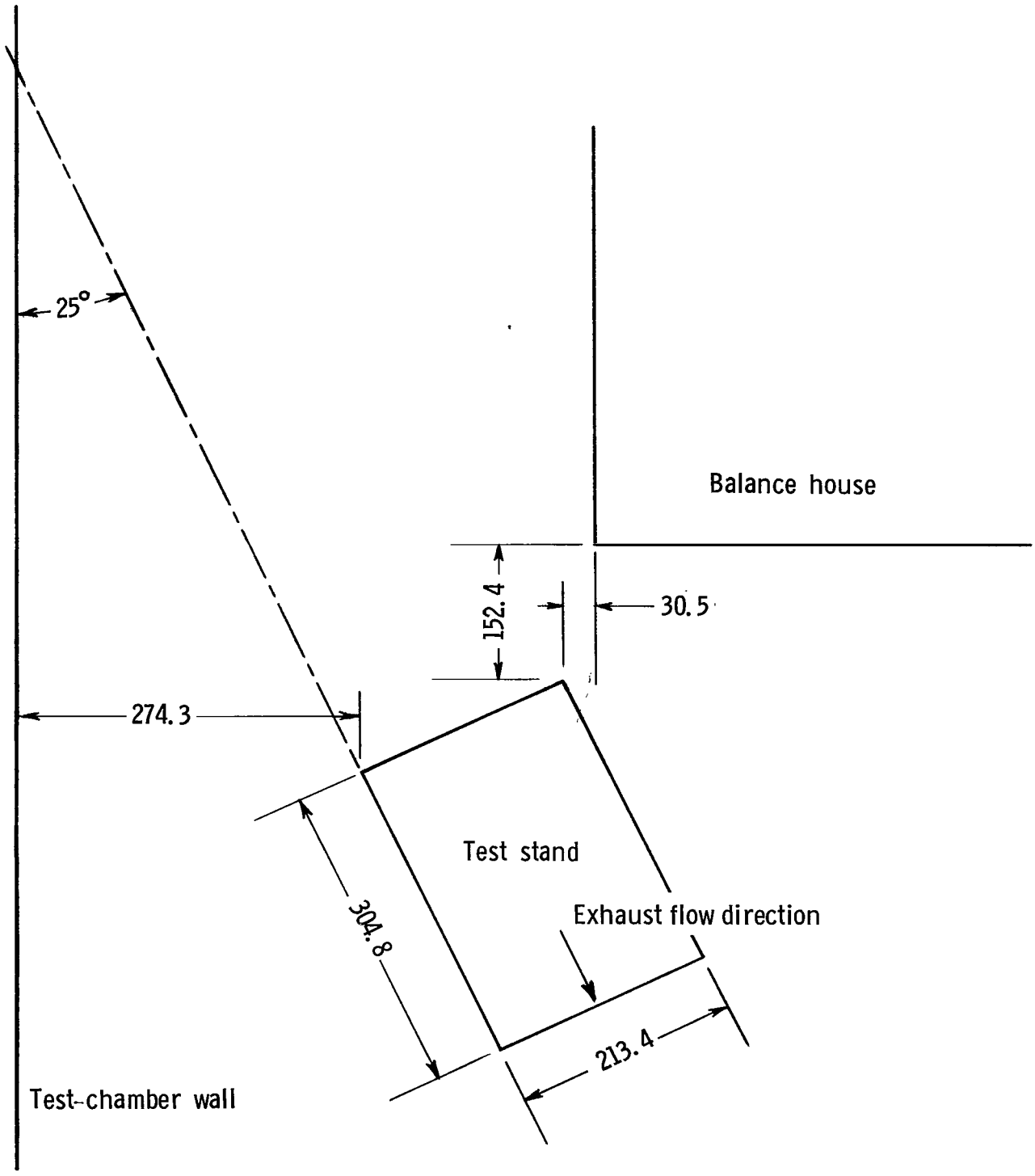

Figure 3.- Schematic drawing showing location of apparatus in test chamber of Langley full-scale tunnel. Dimensions are in centimeters.

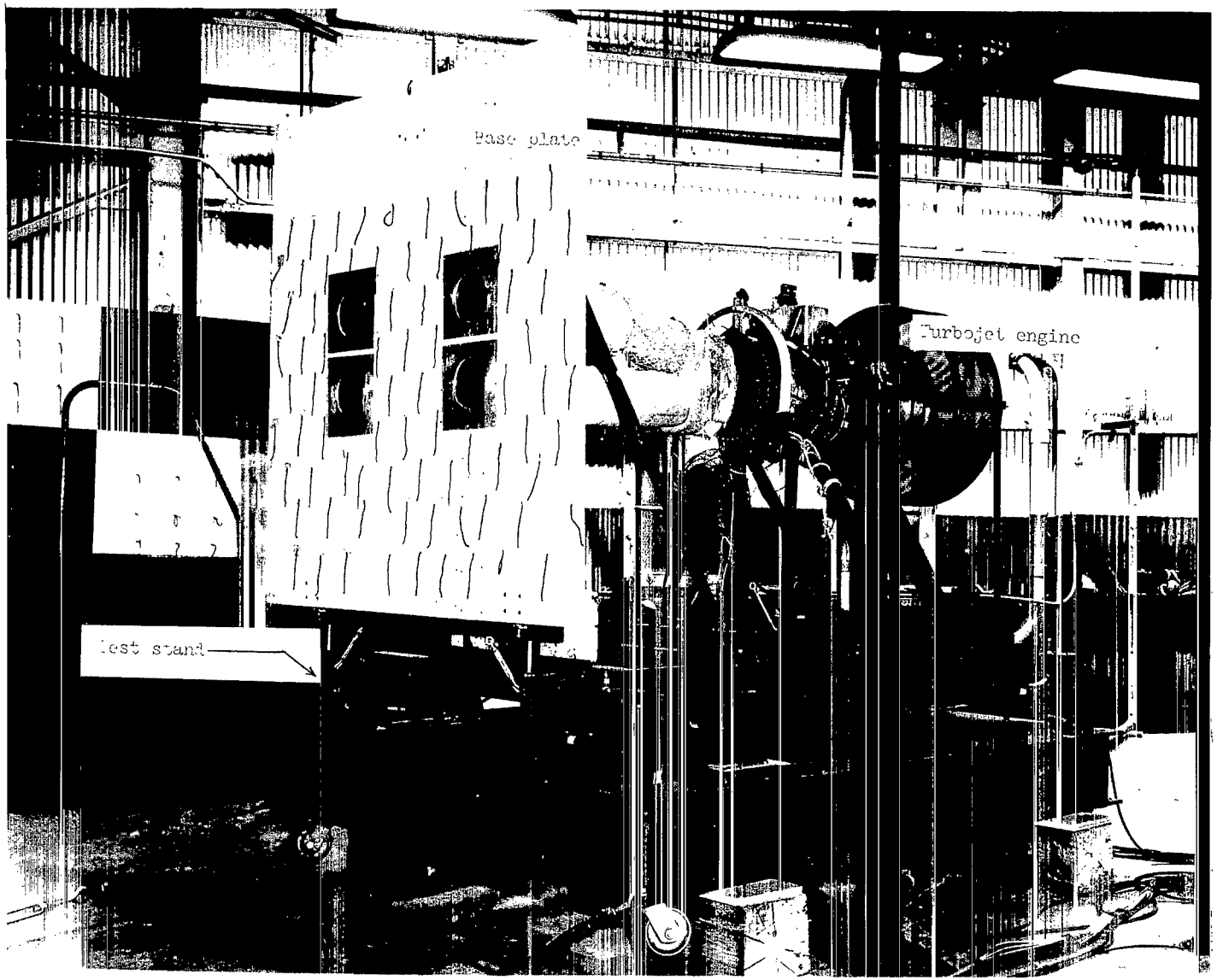

(a) Three-quarter rear view of test apparatus. L-64-10,601.1

Figure 4.- Photographs of four-nozzle exhaust configuration with base plate III installed.

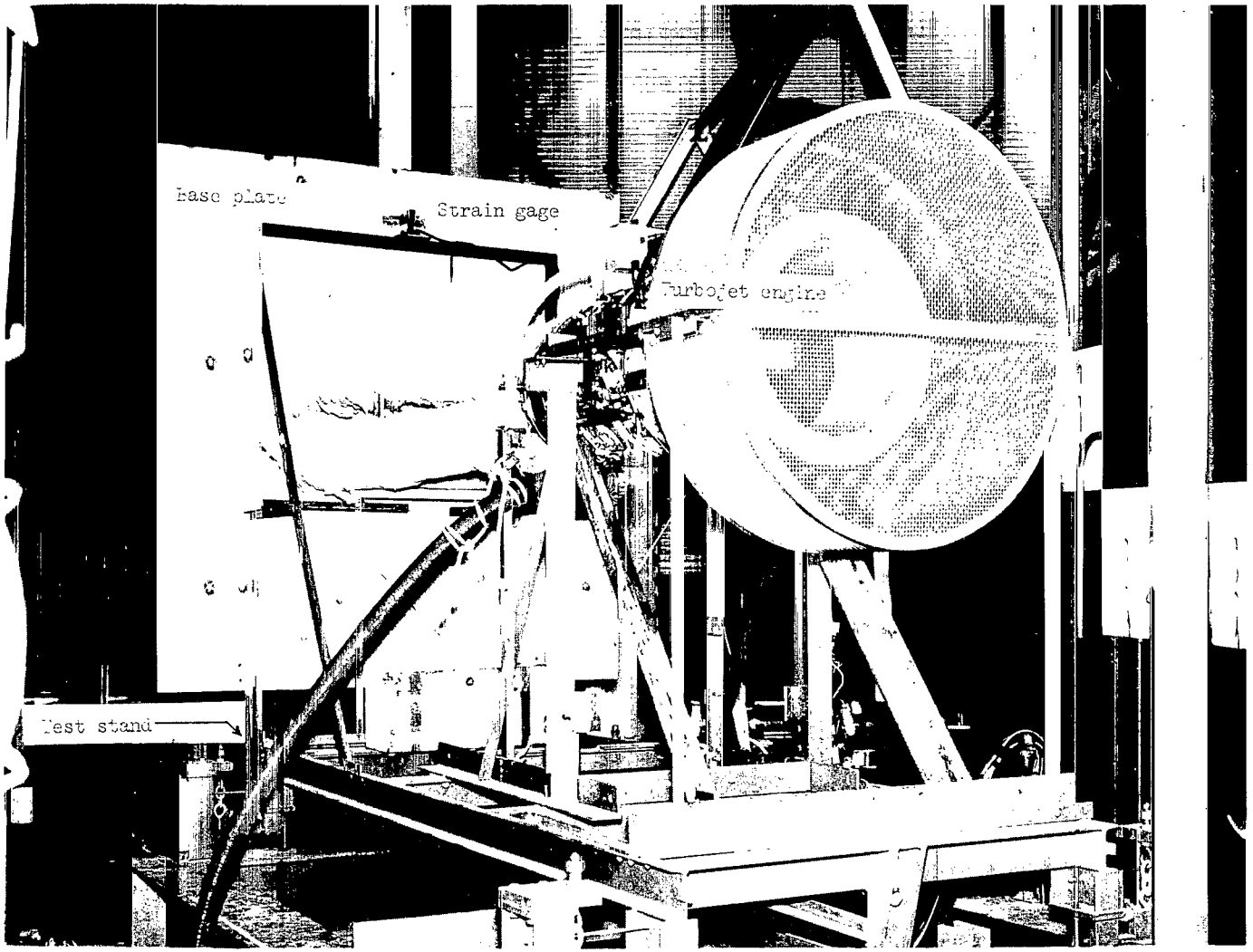

(b) Three-quarter front view of test apparatus. L-64-10,600.1

Figure 4.- Continued.

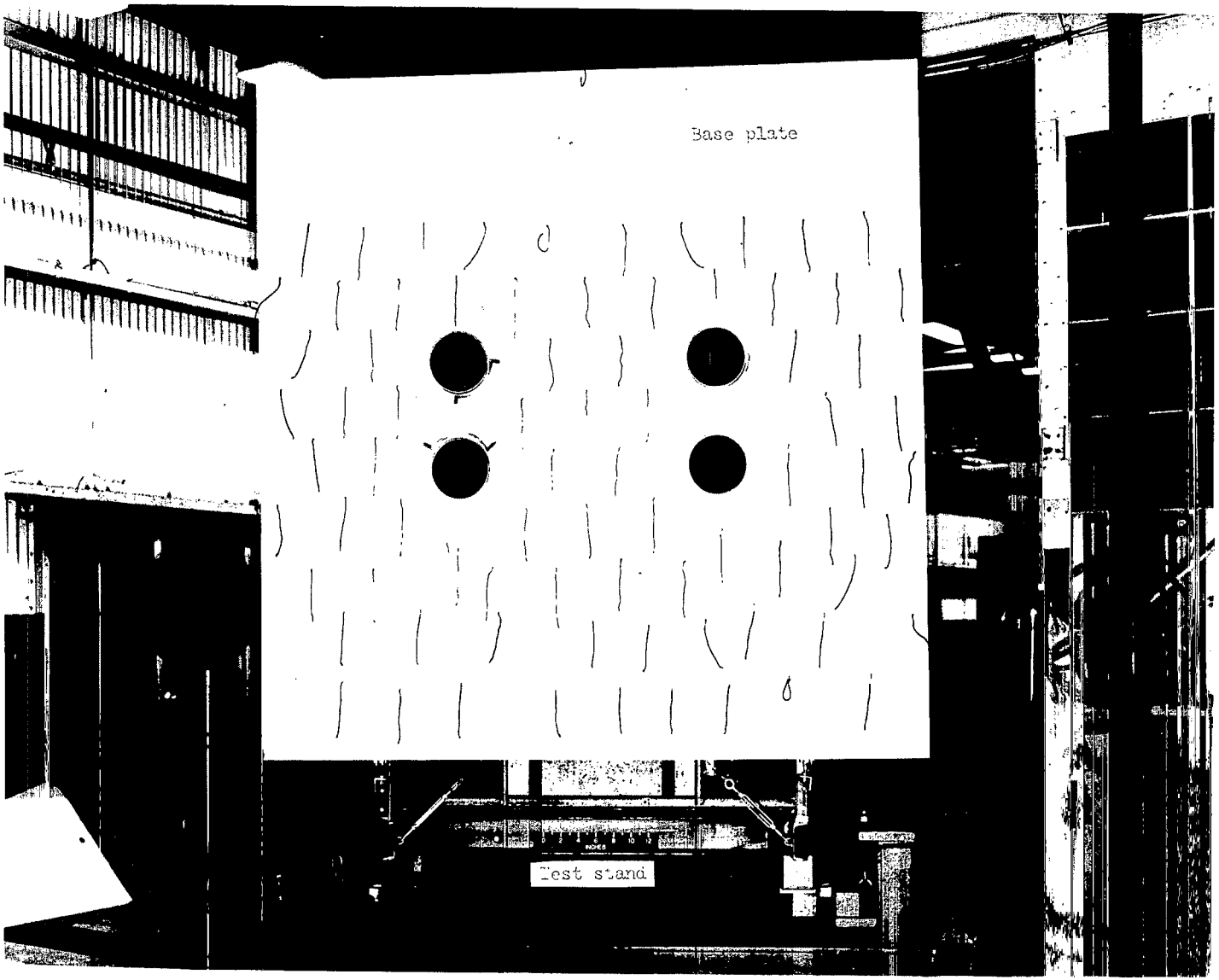

(c) Rear view of test apparatus. L-64-10,602.1

Figure 4.- Concluded.

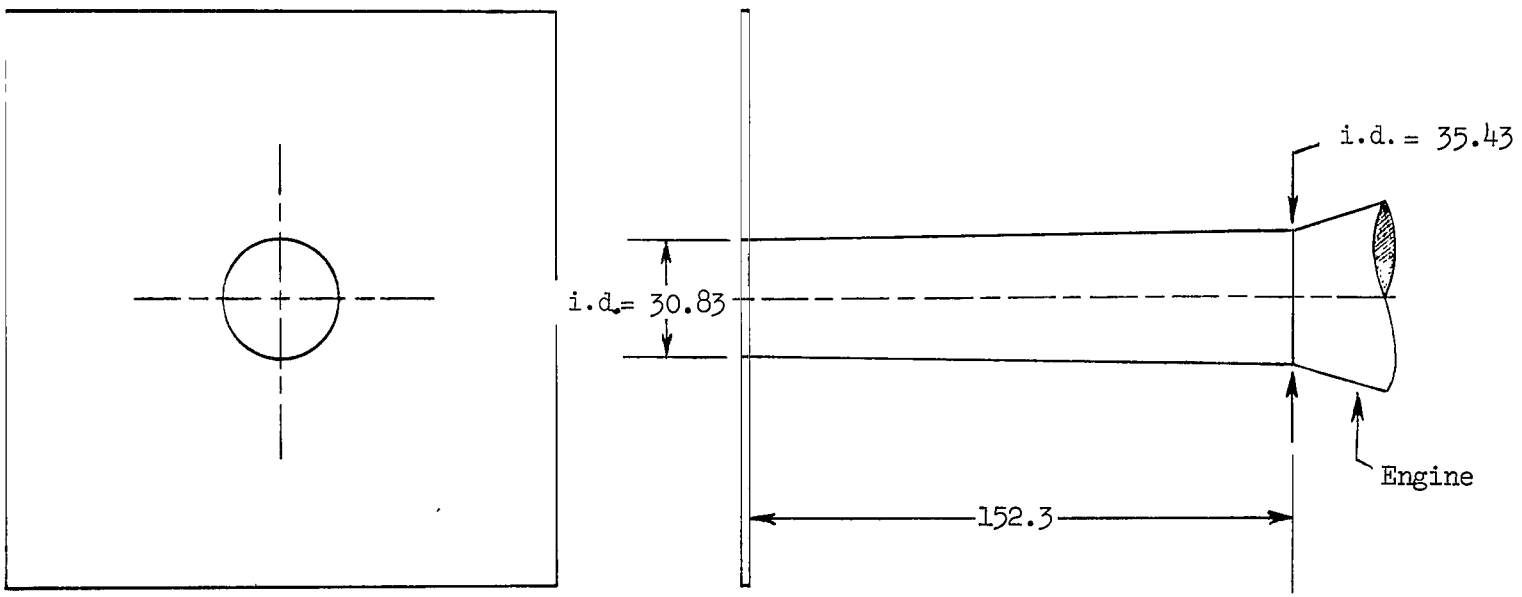

(a) Long-tailpipe single-nozzle configuration with base plate II.

Figure 5.- Tailpipe configurations. Tailpipe at ambient temperature; tailpipes constructed of 0.3-centimeter 347 stainless steel. Dimensions are in centimeters.

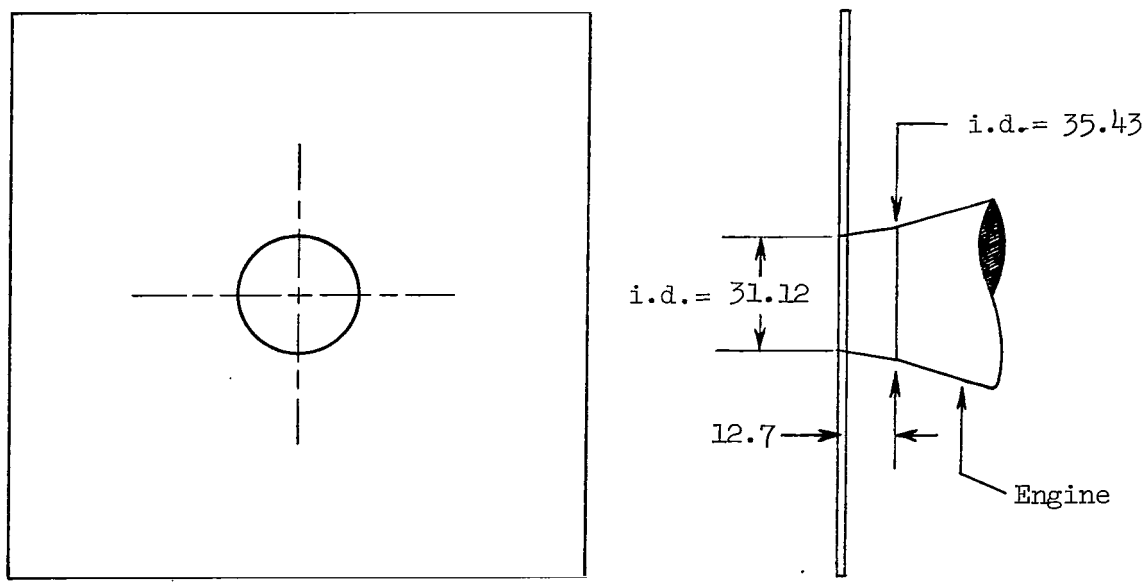

(b) Short-tailpipe single-nozzle configuration with base plate II.

Figure 5.- Continued.

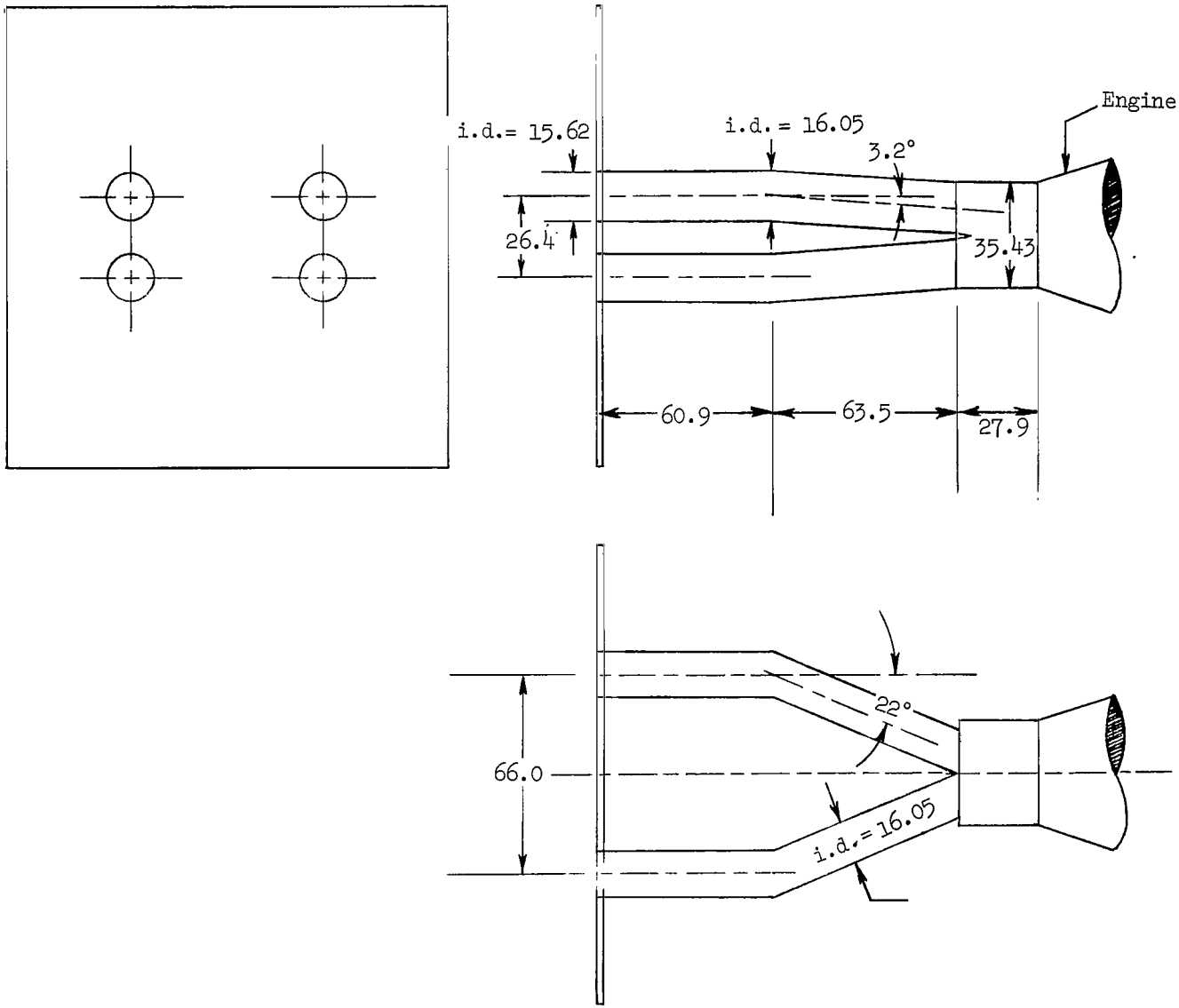

(c) Four-nozzle configuration with base plate II.

Figure 5.- Concluded.

Plywood plate and size	
I	121.8 × 121.8 × 1.9
II	152.3 × 152.3 × 1.9
III	182.8 × 182.8 × 1.9

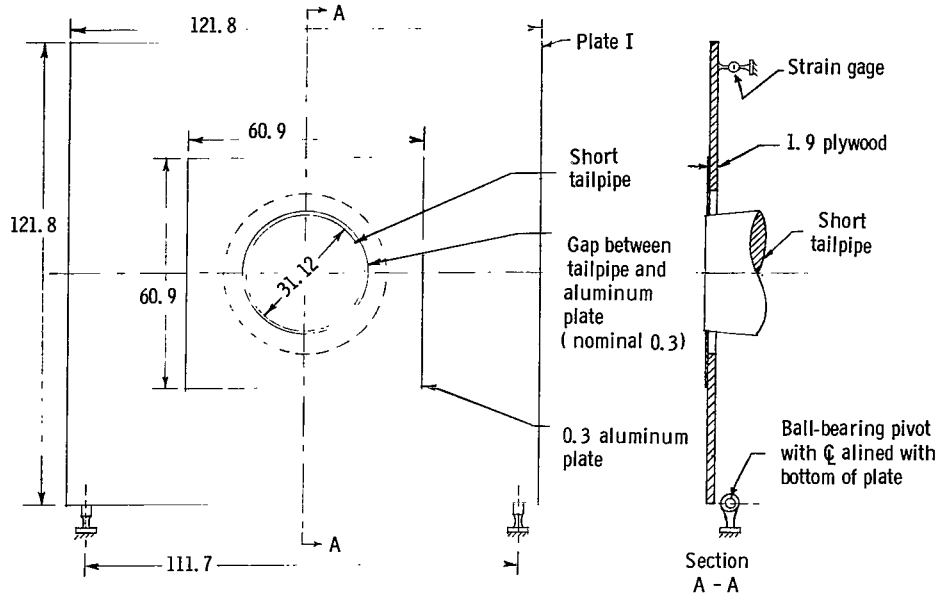

(a) Single-nozzle tailpipe configuration.

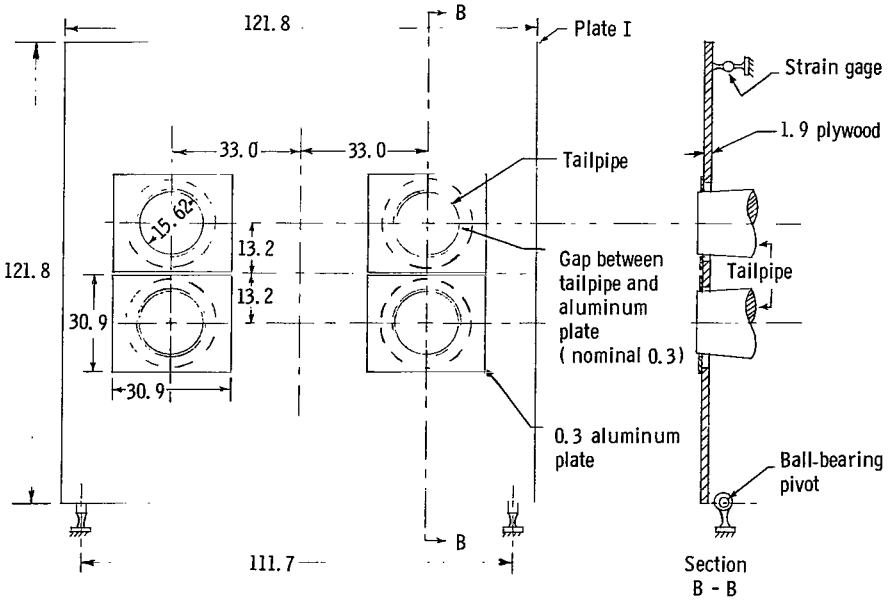

(b) Four-nozzle tailpipe configuration.

Figure 6.- Base plates. Tailpipe at ambient temperatures. Dimensions are in centimeters.

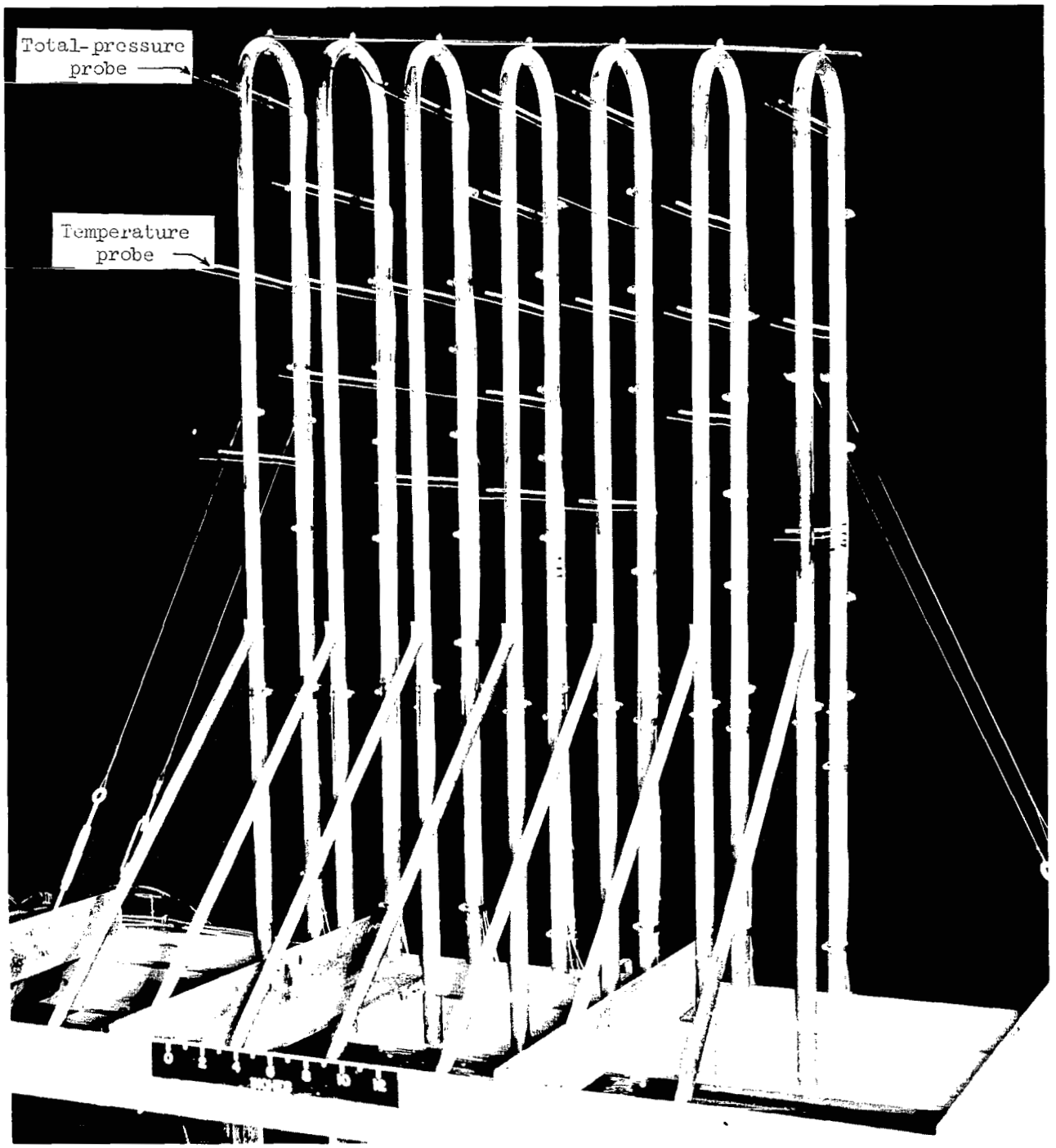

(a) Three-quarter front view of rake. L-65-4273 .1

Figure 7.- Photographs of temperature-pressure exhaust-stream survey rake.

(b) Three-quarter front detail view of temperature-pressure probes. L-65-4272 .1

Figure 7.- Concluded.

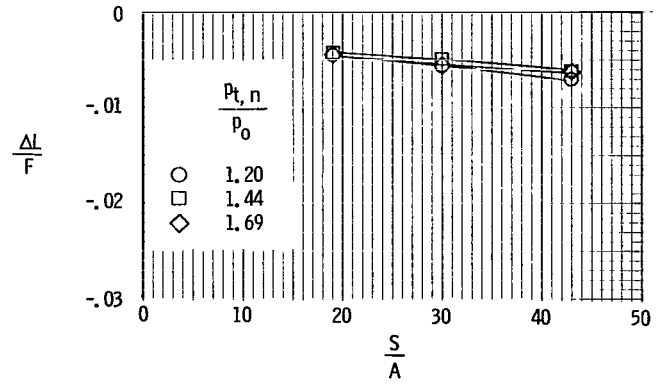

(a) Short-tailpipe single-nozzle configuration.

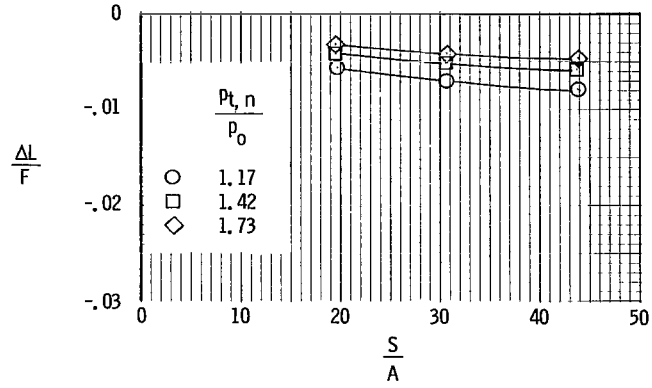

(b) Long-tailpipe single-nozzle configuration.

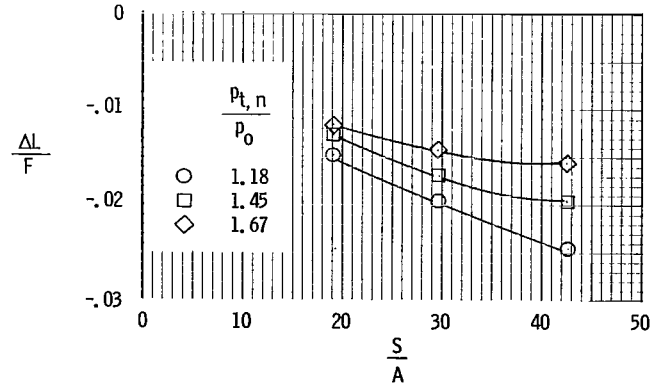

(c) Four-nozzle tailpipe configuration.

Figure 8.- Variation of induced lift loss with plate size for several configurations and pressure ratios.

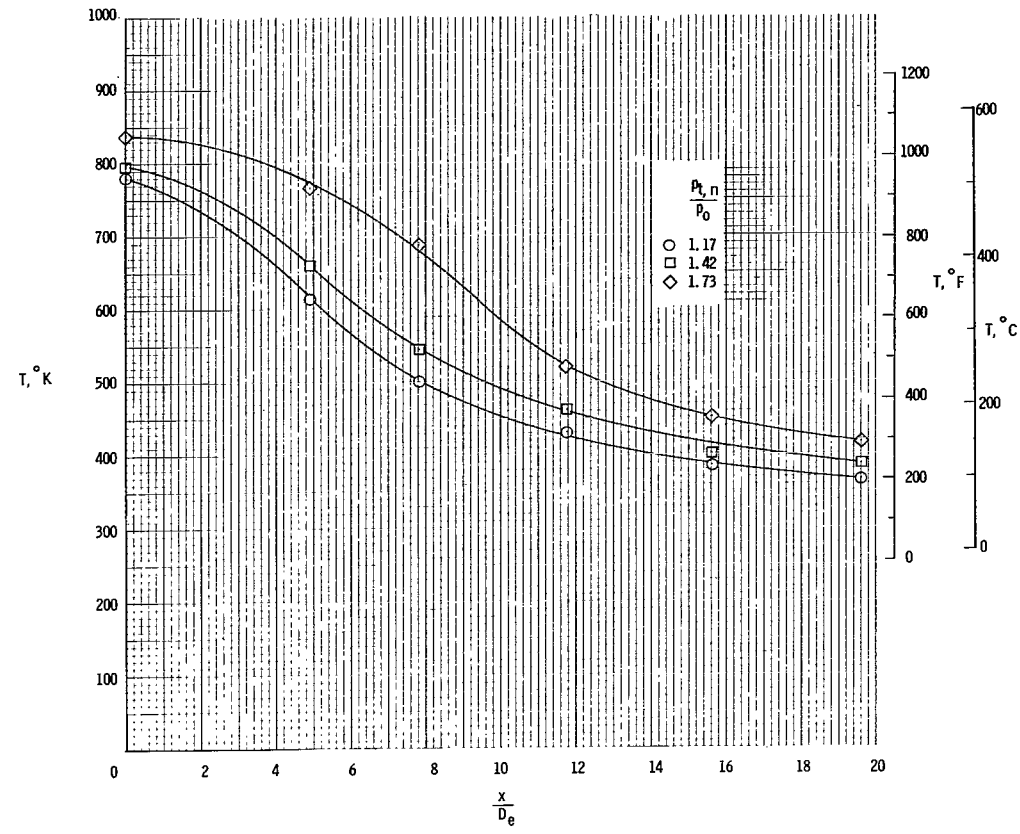

(a) Temperature decay.

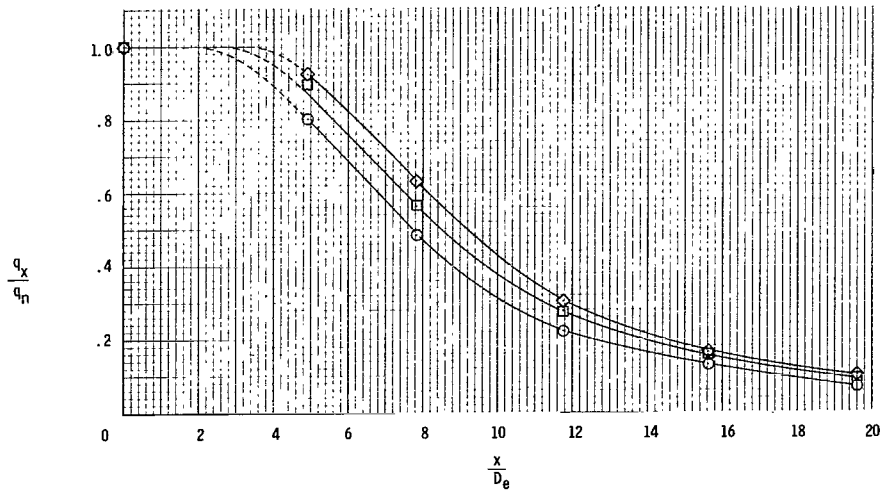

(b) Impact-pressure decay.

Figure 9.- Effect of engine-tailpipe pressure ratio on temperature and impact-pressure decay. Long-tailpipe single-nozzle configuration.

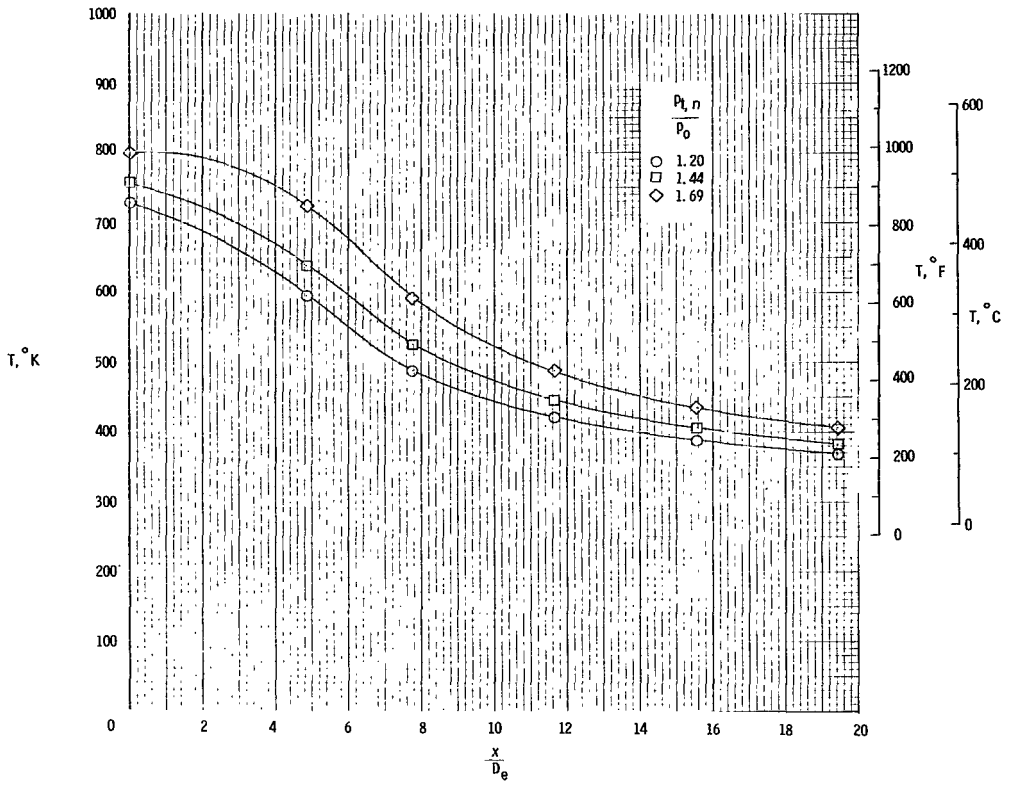

(a) Temperature decay.

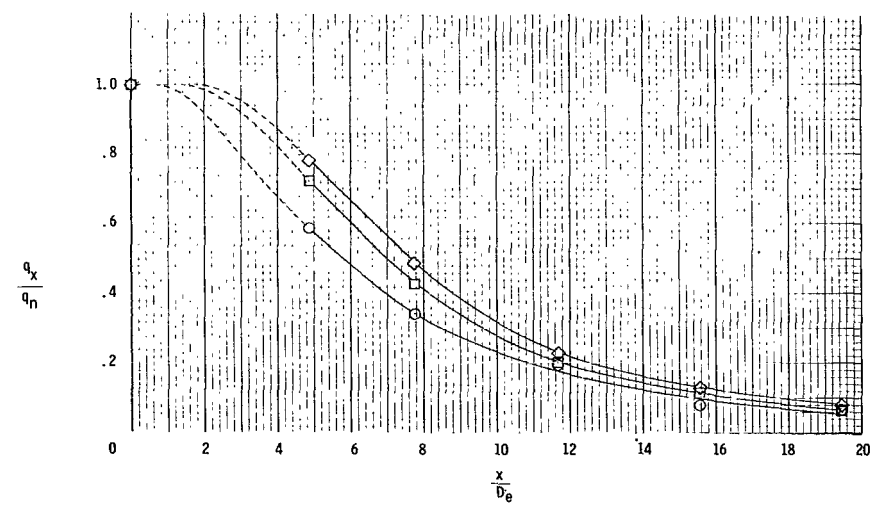

(b) Impact-pressure decay.

Figure 10.- Effect of engine-tailpipe pressure ratio on temperature and impact-pressure decay. Short-tailpipe single-nozzle configuration.

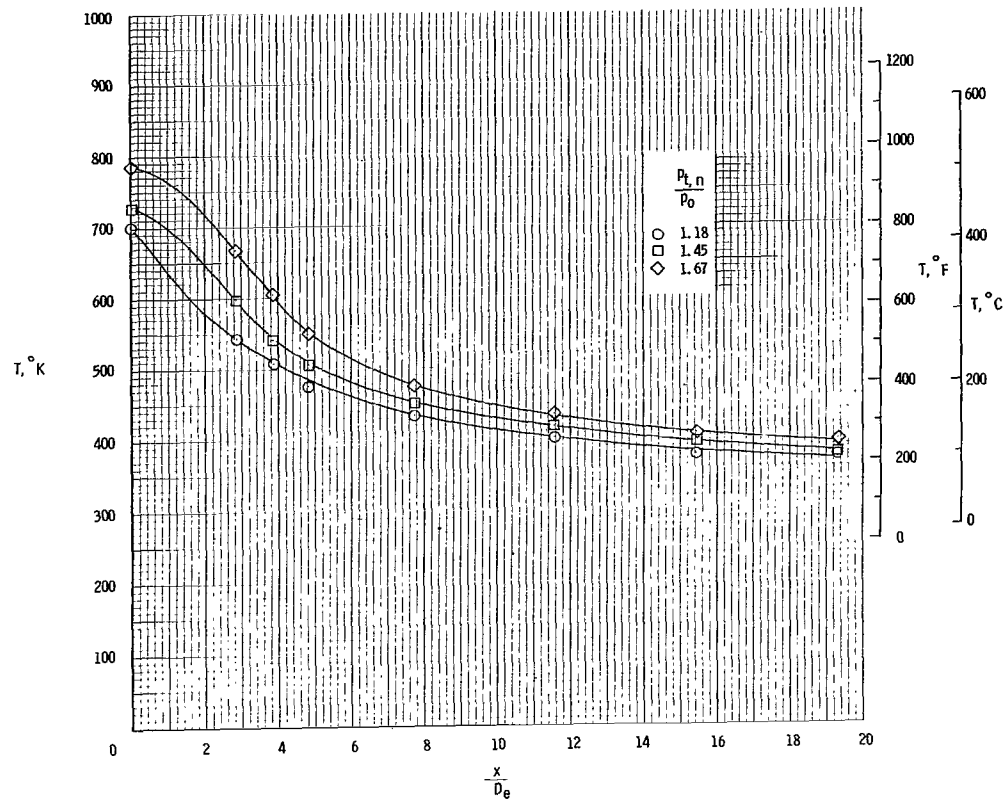

(a) Temperature decay.

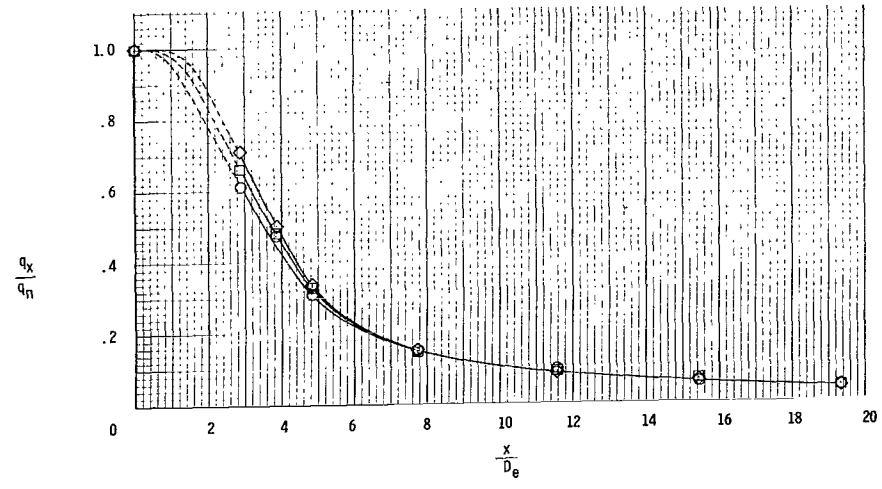

(b) Impact-pressure decay.

Figure 11.- Effect of engine-tailpipe pressure ratio on temperature and impact-pressure decay. Four-nozzle configuration.

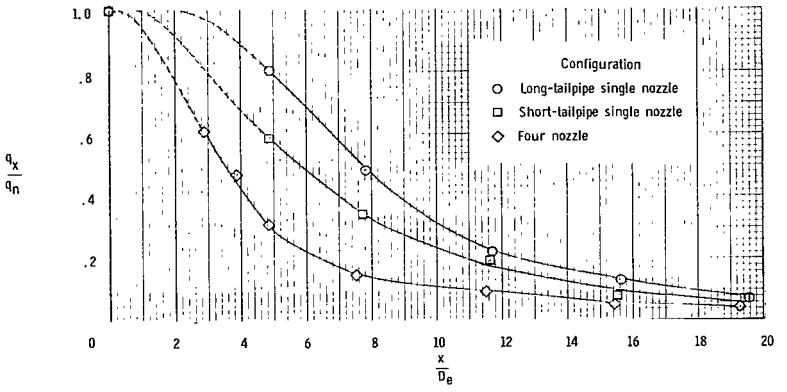

(a) $\frac{p_{t,n}}{p_0} \approx 1.2$.

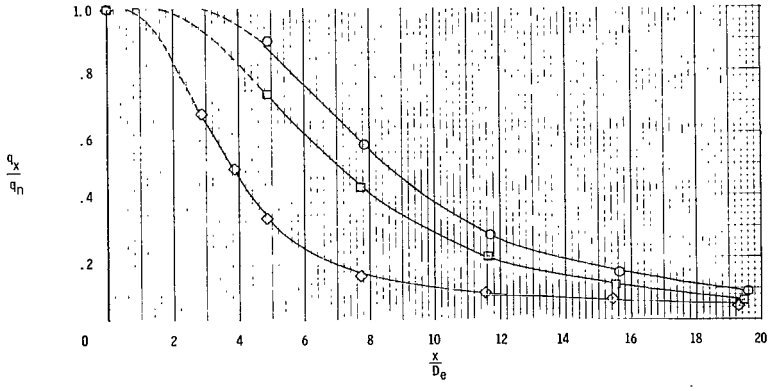

(b) $\frac{p_{t,n}}{p_0} \approx 1.4$.

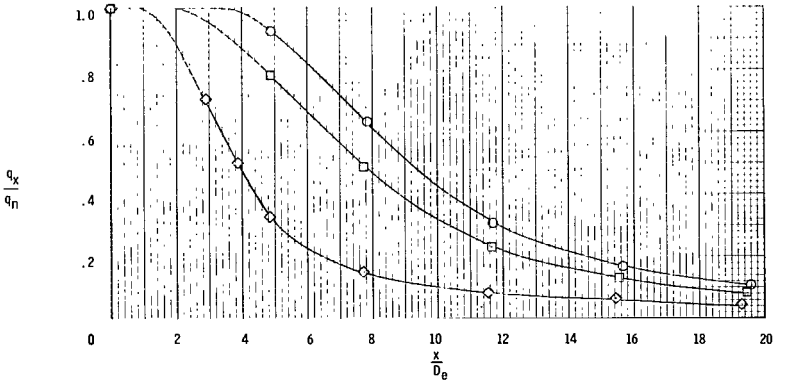

(c) $\frac{p_{t,n}}{p_0} \approx 1.7$.

Figure 12.- Effect of nozzle configuration on impact-pressure decay characteristics.

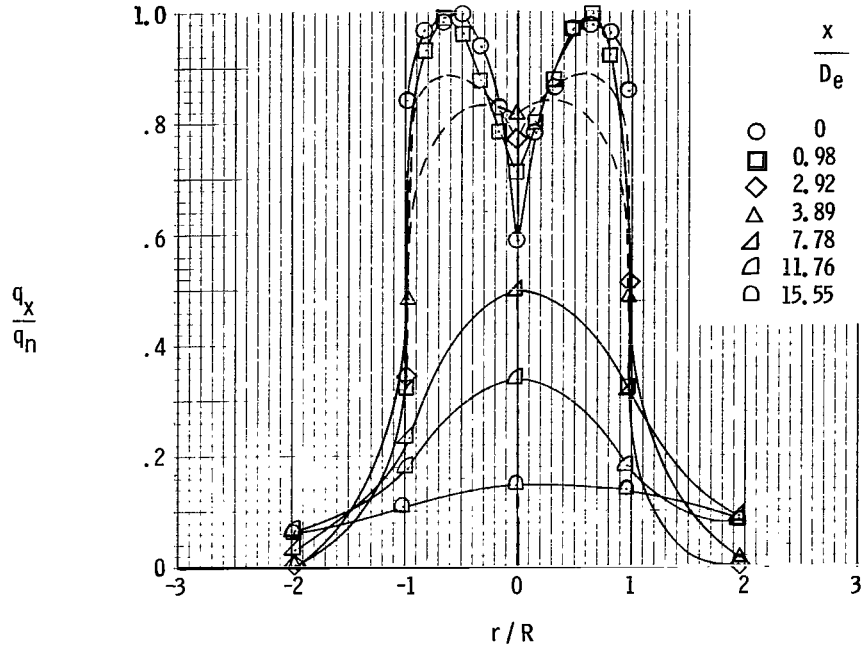

(a) Short-tailpipe single-nozzle configuration; $p_{t,n}/p_0 = 1.69$.

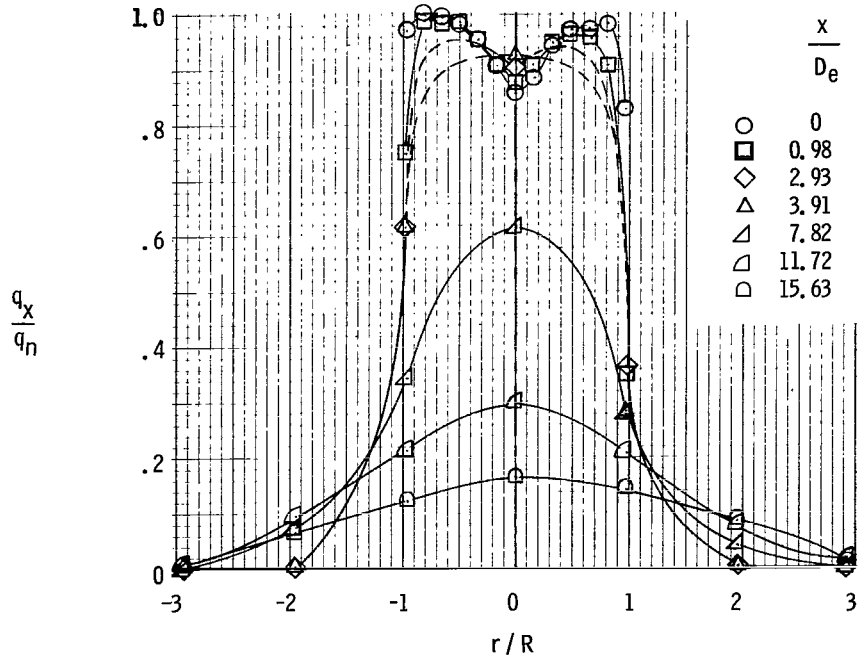

(b) Long-tailpipe single-nozzle configuration; $p_{t,n}/p_0 = 1.73$.

Figure 13.- Engine-exhaust impact-pressure characteristics of two configurations at several downstream locations. (Dashed lines indicate assumed fairing.)

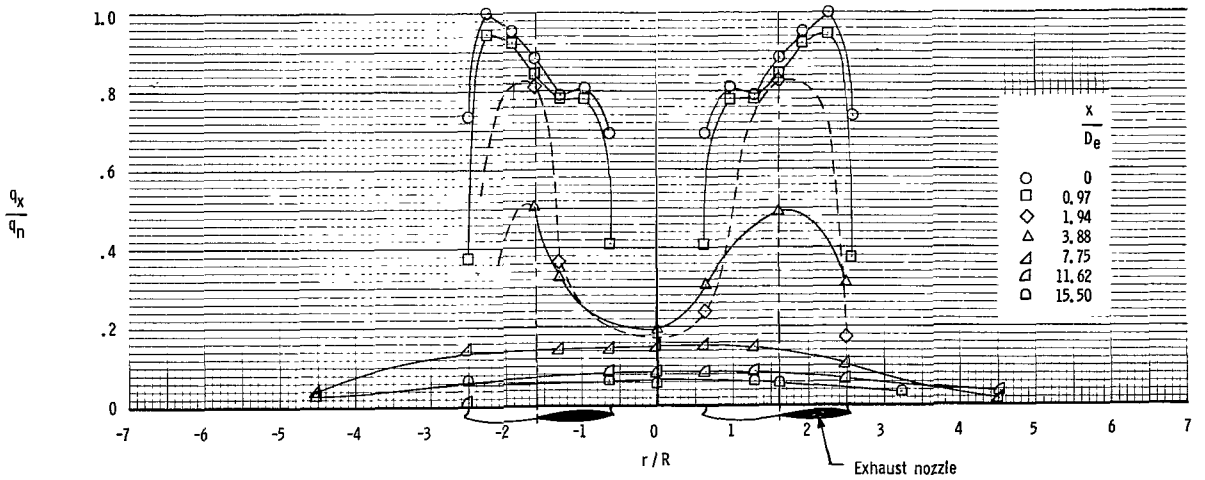

(a) Section A-A.

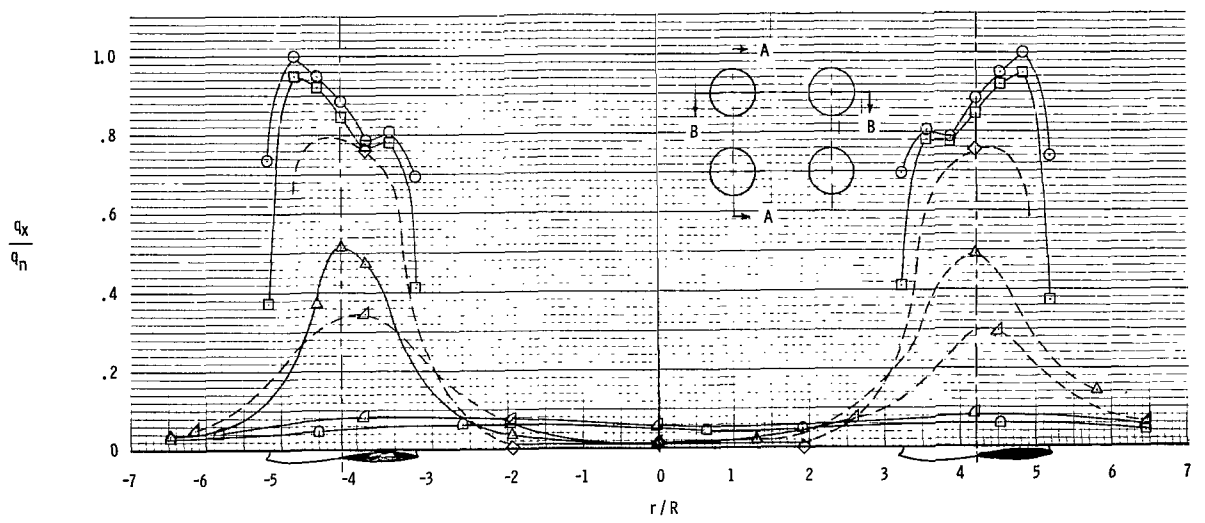

(b) Section B-B.

Figure 14.- Engine-exhaust impact-pressure characteristics of four-nozzle configuration at several downstream locations. $p_{t,n}/p_0 = 1.67$. (Dashed lines indicate assumed fairing.)

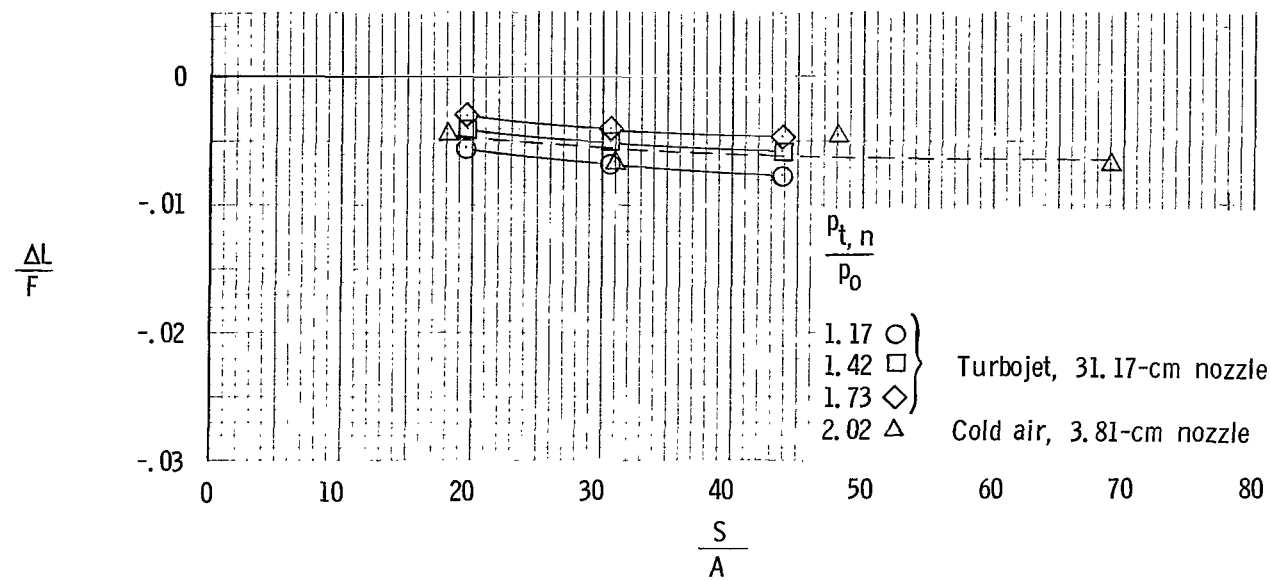

(a) Long-tailpipe single-nozzle configuration.

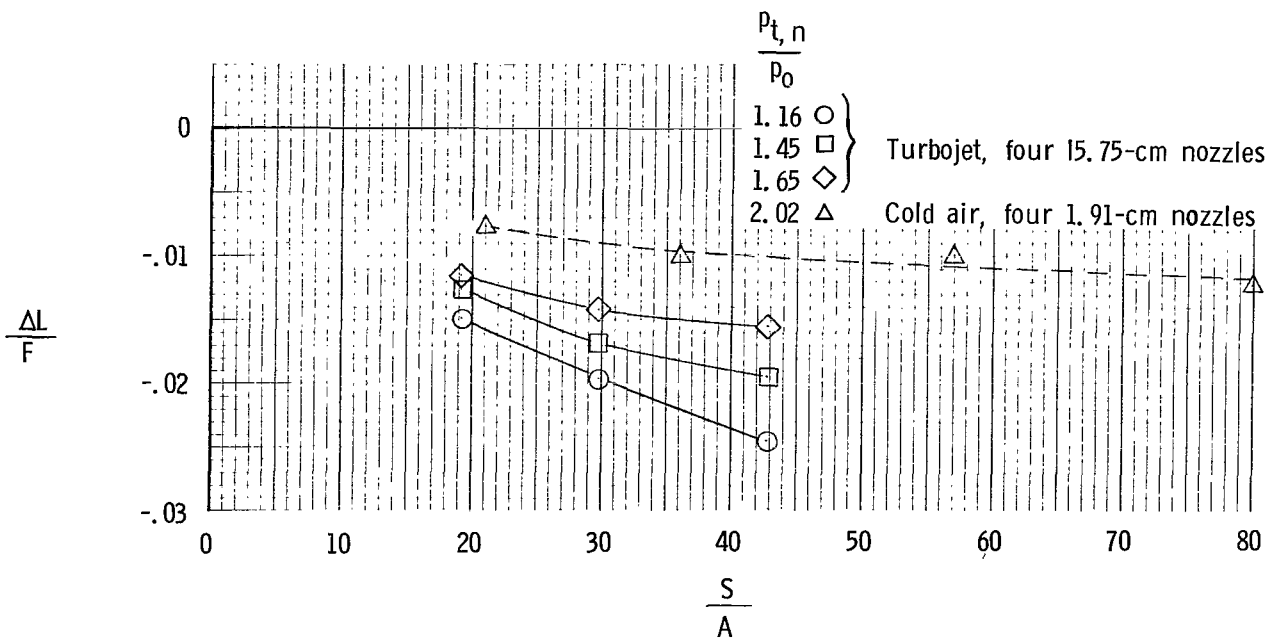

(b) Four-nozzle configuration.

Figure 15.- Comparison of turbojet and small-scale geometrically similar configurations.

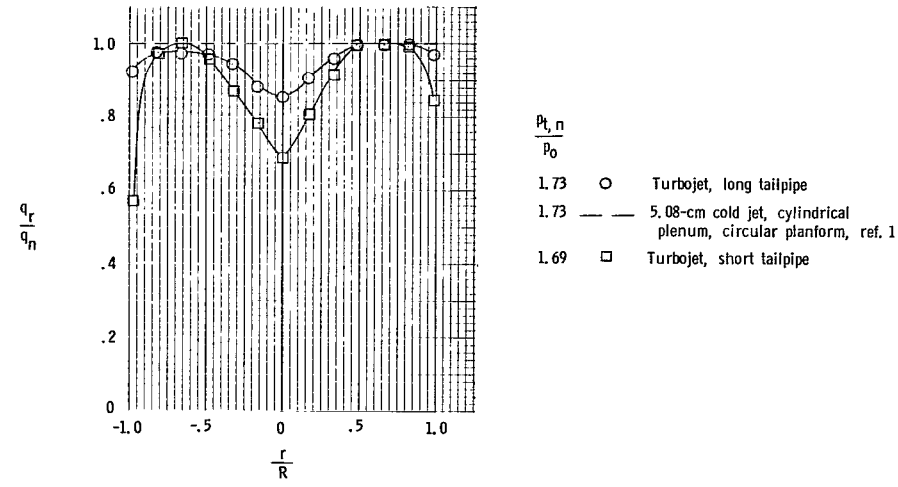

(a) Nozzle survey.

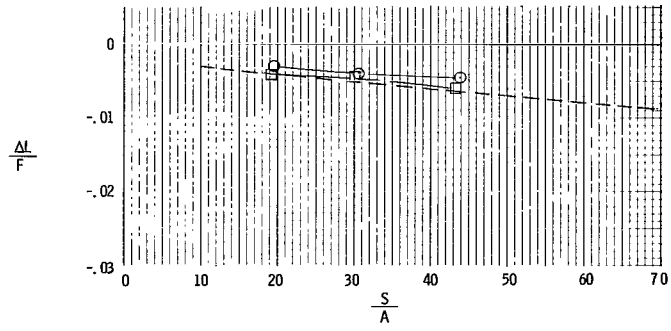

(b) Induced lift loss.

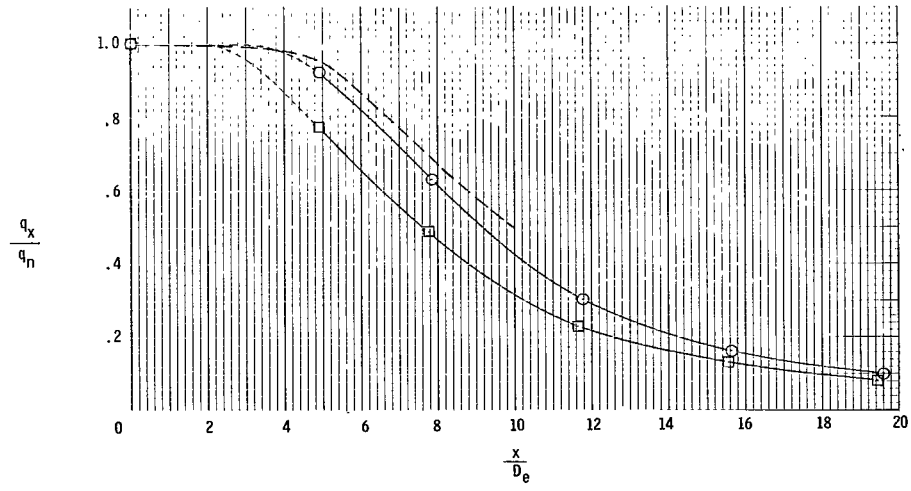

(c) Impact-pressure decay.

Figure 16.- Comparison of several parameters of turbojet results with those obtained during a small-scale, cold-jet investigation of reference 1. Single-nozzle configurations.

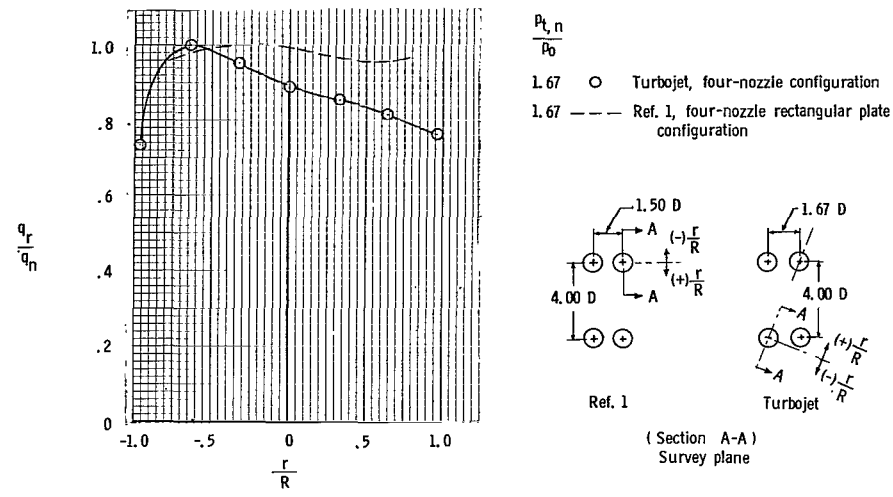

(a) Nozzle survey.

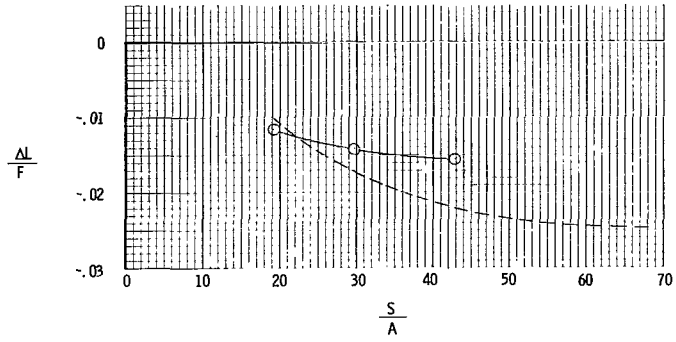

(b) Induced lift loss.

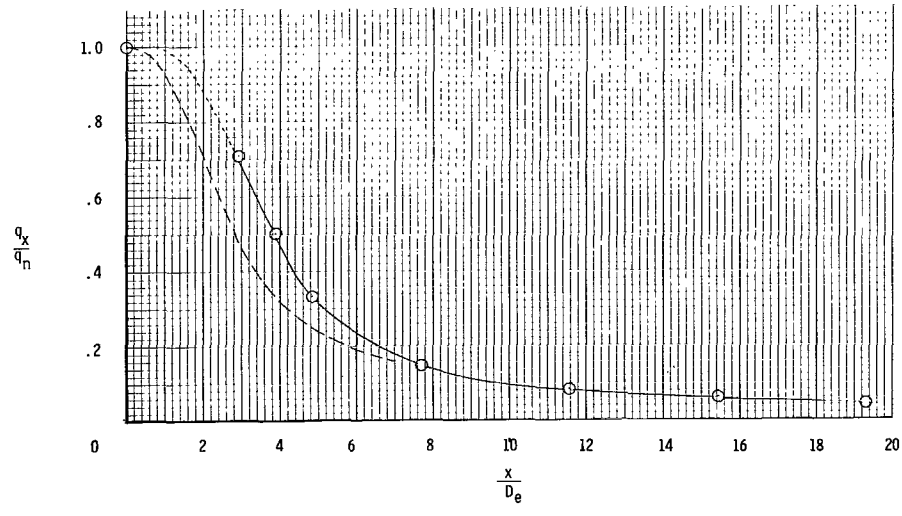

(c) Impact-pressure decay.

Figure 17.- Comparison of several parameters of turbojet results with those obtained during a small-scale, cold-jet investigation of reference 1. Four-nozzle configuration.

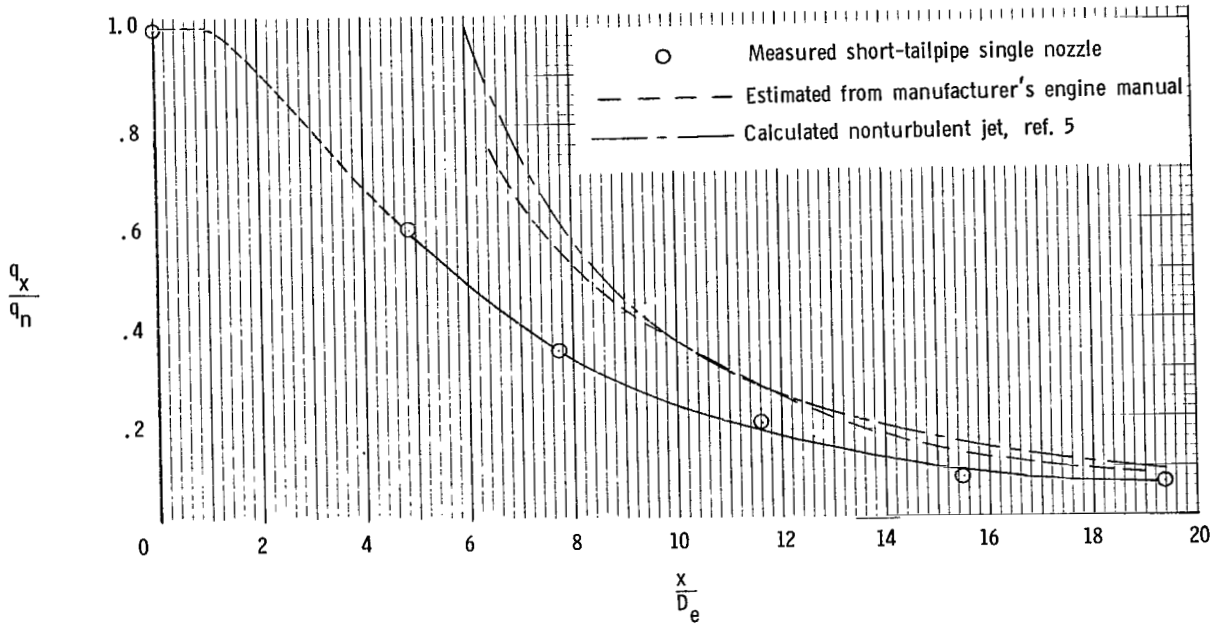

(a) $\frac{p_{t,n}}{p_0} \approx 1.2$.

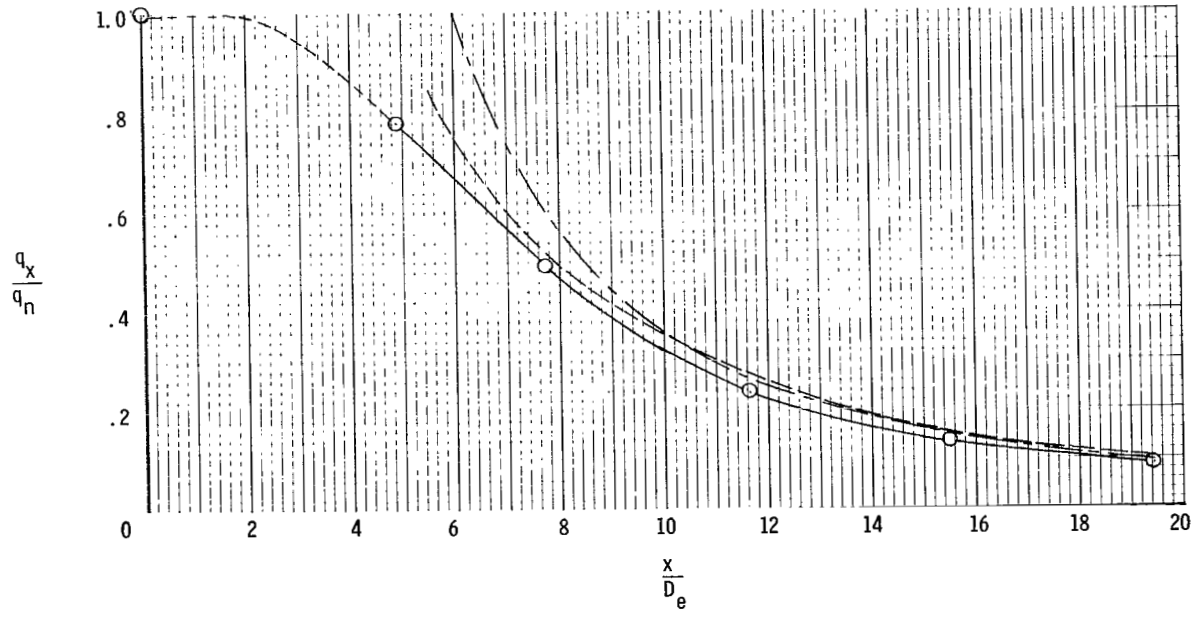

(b) $\frac{p_{t,n}}{p_0} \approx 1.7$.

Figure 18.- Comparison of measured and estimated exhaust impact-pressure decay.

"The aeronautical and space activities of the United States shall be conducted so as to contribute . . . to the expansion of human knowledge of phenomena in the atmosphere and space. The Administration shall provide for the widest practicable and appropriate dissemination of information concerning its activities and the results thereof."

—NATIONAL AERONAUTICS AND SPACE ACT OF 1958

NASA SCIENTIFIC AND TECHNICAL PUBLICATIONS

TECHNICAL REPORTS: Scientific and technical information considered important, complete, and a lasting contribution to existing knowledge.

TECHNICAL NOTES: Information less broad in scope but nevertheless of importance as a contribution to existing knowledge.

TECHNICAL MEMORANDUMS: Information receiving limited distribution because of preliminary data, security classification, or other reasons.

CONTRACTOR REPORTS: Technical information generated in connection with a NASA contract or grant and released under NASA auspices.

TECHNICAL TRANSLATIONS: Information published in a foreign language considered to merit NASA distribution in English.

TECHNICAL REPRINTS: Information derived from NASA activities and initially published in the form of journal articles.

SPECIAL PUBLICATIONS: Information derived from or of value to NASA activities but not necessarily reporting the results of individual NASA-programmed scientific efforts. Publications include conference proceedings, monographs, data compilations, handbooks, sourcebooks, and special bibliographies.

Details on the availability of these publications may be obtained from:

SCIENTIFIC AND TECHNICAL INFORMATION DIVISION

NATIONAL AERONAUTICS AND SPACE ADMINISTRATION

Washington, D.C. 20546